Cameca News (Cameca Instruments Inc., Trumbull, CT, 1987), pp. 1–6.
38. A. L. Graham, A. W. R. Bevan, R. Hutchison, *Catalogue of Meteorites* (Univ. of Arizona Press, Tuscon, AZ, 1985).
39. R. N. Clayton, T. K. Mayeda, J. N. Goswami, E. J. Olsen, *Terra Cognita* **6**, 130 (1986).
40. We gratefully acknowledge the laboratory assistance of C. Coath, C. Engrand, and G. Jarzebinski. The manuscript was improved by constructive comments from two anonymous reviewers. Supported by NASA grants NAG5-4704 (K.D.M.) and NAGW-3553 (G.J.M.).

9 October 1997; accepted 3 March 1998

Osmium Isotopic Evidence for Ancient Subcontinental Lithospheric Mantle Beneath the Kerguelen Islands, Southern Indian Ocean

Deborah R. Hassler and Nobumichi Shimizu

Upper mantle xenoliths found in ocean island basalts are an important window through which the oceanic mantle lithosphere may be viewed directly. Osmium isotopic data on peridotite xenoliths from the Kerguelen Islands, an archipelago that is located on the northern Kerguelen Plateau in the southern Indian Ocean, demonstrate that pieces of mantle of diverse provenance are present beneath the Islands. In particular, peridotites with unradiogenic osmium and ancient rhenium-depletion ages (to 1.36×10^9 years old) may be pieces of the Gondwanaland subcontinental lithosphere that were incorporated into the Indian Ocean lithosphere as a result of the rifting process.

The Kerguelen hotspot became active at least 115 million years ago (Ma) (*1*), and possibly as long as 130 Ma, when India separated from Australia-Antarctica (*2*). The Kerguelen mantle plume is considered to be responsible for extensive hotspot volcanism in the Indian Ocean basin (*3*), including the Ninetyeast Ridge, Broken Ridge, and the Kerguelen Plateau, the second largest of the oceanic plateaus (Fig. 1). Moreover, the Kerguelen plume is a carrier of the DUPAL isotopic anomaly (*4*), a characteristic of basalts erupted in the Southern Hemisphere. The interaction of this plume with the Indian Ocean lithosphere has potentially affected the geochemical and tectonic evolution of the entire Indian Ocean basin (*2*, *5*).

One notion for the origin of the Kerguelen Plateau and the Kerguelen Islands is that their lithospheric basement contains a continental fragment left behind from the breakup of Gondwanaland (*6*). Basalts from the southern Kerguelen Plateau (Ocean Drilling Project drill site 738) do have trace element and isotopic signatures indicative of a continental component in their source (*7*), and recent seismic experiments showed that the southern Kerguelen Plateau has a structure similar to that of a continental passive margin (*8*). However, a seismic refraction study, as well as early isotopic work on basalts from the archipelago, established an apparent oceanic origin (*6*, *9*). Here we present Os isotopic data that establish the presence of continental lithosphere in the northern Kerguelen Plateau and the involvement of continental materials in the formation of the Kerguelen Islands.

We examined the Re-Os isotopic systematics in peridotite xenoliths (*10*) from two sample localities that are less than 10 km apart (Lac Superieur and Mont Trapeze) in the Courbet Peninsula, northeastern Kerguelen Islands (Fig. 1, inset). The xenoliths are abundant in alkaline basaltic dikes that cross-cut "plateau basalt" lavas that comprise the Courbet Peninsula and formed 23 to 25 million years ago (Ma) (*11*).

The samples are predominantly refractory coarse granular harzburgites [olivine: ~60% (forsterite content = 90 to 92%); orthopyroxene: ~35%; clinopyroxene: 1 to 5%; and trace amounts of spinel], but also include more clinopyroxene-rich lherzolites and wehrlitic-dunites. The rocks are fresh and do not contain any secondary alteration minerals. Many of the peridotites (from both localities) reacted with melts that percolated through them. For example, some harzburgites contain newly formed clinopyroxene crystals that are enriched in incompatible trace elements (for example, chondrite normalized $La_N = 100$), whereas coexisting original clinopyroxene grains occur as symplectite intergrowths with both orthopyroxene and spinel and have depleted incompatible trace element abundances (for example, $La_N = 3$). Some peridotites at more advanced stages of reaction have trace element–enriched clinopyroxenes (for example, $La_N = 300$) that are intergrown with phlogopite (*12*).

During interactions with percolating metasomatic melts, the Sr and Nd isotopic characteristics of the original peridotites are likely to be replaced by those of the melt, because the concentrations of these incom-

Table 1. Rhenium and osmium isotopic results from Kerguelen Islands peridotite xenoliths. All samples are spinel harzburgites except as noted. ND, not determined.

Sample	$^{187}Os/^{188}Os$	Os (*33*) (ppt)	Re (ppt)	Re/Os ($\times 10^{-3}$)	T_{RD} (*25*) (Ga)
		Lac Superieur			
OB93-51*	0.1262 ± 2	87	ND		
OB93-52†	0.1286 ± 3	4218	ND		
OB93-64‡	0.1300 ± 2	968	ND		
OB93-77	0.1263 ± 3	3199	5	2	
OB93-78	0.1266 ± 6	2888	ND		
OB93-80	0.1252 ± 2	1727	ND		
OB93-82‡	0.1287 ± 2	6999	ND		
OB93-83*§	0.1257 ± 4	44	ND		
		Mont Trapeze			
OB93-280	0.1189 ± 2	3067	6	2	1.36
OB93-284	0.1236 ± 1	6652	29	4	0.63
OB93284b‖	0.1229 ± 3	6645	ND		0.74
OB93-287	0.1239 ± 3	1267	49	39	0.58
OB93-289	0.1224 ± 3	3411	12	4	0.81
OB93-291	0.1205 ± 4	2157	11	5	1.11
OB93-297	0.1228 ± 3	2409	31	13	0.75
OB93-305	0.1211 ± 3	2012	72	36	1.02
OB93-305r‖	0.1202 ± 4	2179	ND		1.16
OB93-306	0.1276 ± 5	516	41	80	
OB93-307	0.1229 ± 3	5605	49	9	0.74
OB93-314	0.1383 ± 6	3281	9	3	
OB93-317	0.1196 ± 4	2652	11	4	1.25

*Olivine separate. †Spinel lherzolite. ‡Wehrlitic dunite. §Phologpite-bearing spinel lherzolite. ‖Replicate.

D. R. Hassler, Massachusetts Institute of Technology–Woods Hole Oceanographic Institution, Joint Program in Oceanography, Department of Geology and Geophysics, Woods Hole Oceanographic Institution, Woods Hole, MA 02543, USA.
N. Shimizu, Department of Geology and Geophysics, Woods Hole Oceanographic Institution, Woods Hole, MA 02543, USA.

patible elements in the melt are much higher than in the peridotite. For example, Sr isotopic compositions of clinopyroxenes from the few unmetasomatized peridotite xenoliths (for example, OB93-78: $^{87}Sr/^{86}Sr$ = 0.70329 ± 2) are similar to those of Indian mid-ocean ridge basalts [MORB (*13*)], whereas metasomatic clinopyroxenes have Sr isotopic compositions (for example, OB93-83: $^{87}Sr/^{86}Sr$ = 0.706427 ± 10) similar to those of alkaline basalts from the Kerguelen Islands (*6*), reflecting their origin from Kerguelen plume melts (*12*, *14*). Thus, the incompatible geochemical tracers record mantle processes associated with plume-lithosphere interaction, but information about xenolith provenance is lost in the xenoliths that have undergone metasomatic reaction.

In contrast, the isotopic compositions of elements that are compatible in peridotites are less likely to be modified during metasomatism because their concentrations are much higher in peridotites than in the percolating melts. Osmium is a compatible element during partial melting of peridotite (*15*); therefore, ^{187}Os, the radiogenic daughter of ^{187}Re, is an isotopic tracer that is relatively insensitive to subsequent mantle metasomatic processes. For these reasons, the Re-Os system is particularly suitable for determining the provenance of peridotites and for dating primary melting events of peridotite formation (*16*).

The Os isotopic compositions of peridotite xenoliths from the Kerguelen Islands (Table 1 and Fig. 2) vary over a wide range ($^{187}Os/^{188}Os$ = 0.1189 ± 2 to 0.1383 ± 6) and extend to compositions that are less radiogenic than have been observed in rocks from oceanic settings, including xenoliths from other ocean islands [for example, Samoan peridotites have $^{187}Os/^{188}Os$ = 0.1225 to 0.1309 (*17*)]. Re/Os ratios in the xenoliths are low (2×10^{-3} to 80×10^{-3}; Table 1), and age correction for isotopic ingrowth since the time of the eruption of the host basalts is negligible. The more radiogenic Os isotopic compositions of this xenolith suite cannot be explained by contamination with Kerguelen Islands basalt because unrealistic additions of basalt would be required [>20%; with $^{187}Os/^{188}Os$ = 0.1565, and the concentration of Os = 100 parts per trillion (*18*)]. Thus, we interpret these variations as primary signatures that reflect the diversity of the xenolith provenance.

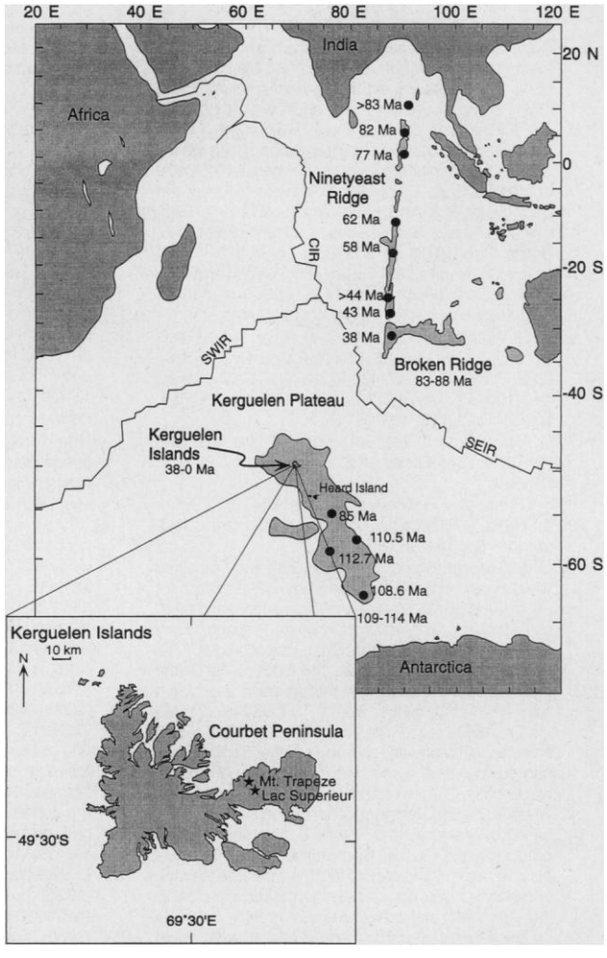

Fig. 1. Map of the Indian Ocean and Kerguelen Islands. Submarine plateaus and ridges related to the Kerguelen Plume are highlighted in light gray shading, and the locations of the SWIR and SEIR are shown. Filled circles correspond to Deep Sea Drilling Project and Ocean Drilling Project drill sites. The ages of recovered basaltic basement for each drill hole are adjacent to the symbols. The Kerguelen Islands (inset) are located at the northern end of the Kerguelen Plateau. On the Courbet Peninsula, asterisks mark the two xenolith localities of this study, Lac Superieur and Mont Trapeze.

Within the sample suite, two spinel harzburgites from Mont Trapeze and three comparatively clinopyroxene-rich lherzolites from Lac Superieur have relatively radiogenic Os isotopic compositions ($^{187}Os/^{188}Os$ = 0.1276 ± 5 to 0.1383 ± 6). These values are typical of ocean island basalts (*19–23*) and may reflect a part of the spectrum of Os isotopic compositions of the Kerguelen plume.

The remaining xenoliths from Lac Superieur are grouped at $^{187}Os/^{188}Os \approx$ 0.1260 ± 7, within the range of compositions estimated for the modern oceanic lithosphere from abyssal peridotites (*19*, *24*). Indeed, some clinopyroxenes in samples of this group have rare earth element abundance patterns comparable to those in abyssal peridotites, and Sr isotopic compositions of clinopyroxenes from these rocks are similar to Indian Ocean MORB values as noted above (*12*). These characteristics are evidence that these xenoliths originated from the Indian Ocean lithospheric mantle.

In contrast, the harzburgites from Mont Trapeze exhibit a greater range in Os isotopic composition, and most are significantly less radiogenic (to $^{187}Os/^{188}Os$ = 0.1189 ± 2) than the xenoliths from Lac Superieur. Such unradiogenic Os isotopic compositions require reservoirs that had extremely low Re/Os ratios for geologically long periods of time. The Re-depletion model ages (*16*, *25*) for the Mont Trapeze xenoliths are from 0.58×10^9 to 1.36×10^9 years ago (T_{RD}; Table 1). Such unradiogenic Os isotopic compositions have never been observed in oceanic environments and are not expected

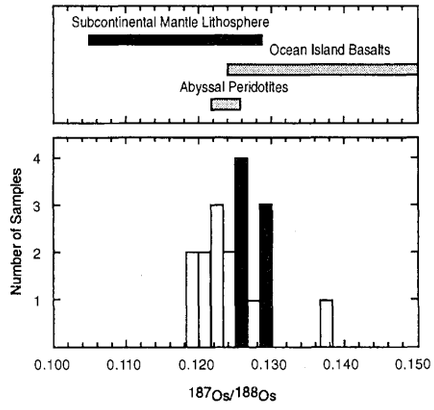

Fig. 2. Histogram of the Os isotopic composition of the Kerguelen Islands peridotite xenoliths by location. Most samples from the Lac Superieur locality (filled bars) are more radiogenic than most of those from the Mont Trapeze locality (open bars). The typical error is less than the width of a bar. Shown for comparison is the range of initial Os isotopic compositions of other rock types from around the world (*16*, *19–24*, *26*, *27*). Only data for abyssal peridotites that are not contaminated with seawater Os are shown.

to be part of the young (~40 Ma beneath the Kerguelen Islands) Indian Ocean mantle lithosphere. Comparably unradiogenic Os isotopic compositions have been found only in ancient subcontinental lithospheric mantle peridotites such as orogenic massifs (*26*) and xenoliths from cratonic areas (*16*, *27*).

We suggest that these anomalous unradiogenic xenoliths are pieces of the Gondwanaland subcontinental lithosphere. That the unradiogenic xenoliths are found in only one of the two localities suggests that the pieces of subcontinental lithosphere could be small and localized and thus undetectable in geophysical observations of the northern Kerguelen Plateau (*9*).

A possible mechanism for emplacing small, discrete fragments of subcontinental lithosphere into the middle of a young ocean basin is that subcontinental lithospheric mantle was delaminated and incorporated into the newly forming Indian Ocean lithosphere during the rifting of the eastern Gondwanaland continents. A similar process may explain the unusual geochemical characteristics of some basalts from the Southwest Indian Ridge (SWIR, 39°E to 41°E), the Afanasy-Nikitin Rise in the northern Indian Ocean, the Oceanographer fracture zone on the Mid-Atlantic Ridge, the geochemical signatures of basalts from the Azores, and the origin of the DUPAL anomaly (*21*, *28*). This process is consistent with the seismic structure of the southern Kerguelen Plateau (*8*). If delamination is common in continental rifting (*29*), it could contribute to mantle heterogeneities that are manifested in basalt geochemistry (*21*, *28*).

Another possibility is that eastern Gondwanaland subcontinental lithospheric mantle was transported to the Kerguelen Plateau by the Kerguelen plume. In this scenario, the convecting incipient plume head eroded the base of the Gondwanaland lithosphere, pieces of which were then integrated into the Indian Ocean lithosphere. The earliest volcanism that can be related to the Kerguelen plume with certainty is the southern Kerguelen Plateau, which formed at 115 Ma (*1*, *30*). At 115 Ma, the Kerguelen Plateau was forming within the young Indian Ocean basin more than 500 km from the Gondwanaland continental margins (*2*, *31*). In this case, an unusually large plume head (diameter = 1000 km) would be required to erode and entrain the Gondwanaland lithosphere into the Kerguelen plume. If the 130-Ma Bunbury Basalts (West Australia) and Rajmahal Traps (India) were identifiable as early Kerguelen plume activities, the requirement for such a large plume head may not be necessary. However, a genetic relationship of these rocks to the plume is still controversial (*30*). On the basis of these arguments, we consider that this model is unlikely.

Alternatively, these unradiogenic xenoliths could be pieces of Precambrian oceanic mantle lithosphere recycled through a subduction zone and returned to the lithosphere by way of the Kerguelen plume. That peridotites with unradiogenic Os isotopic compositions have not yet been observed from any other oceanic islands suggests that this hypothesis, too, is unlikely.

Our present data suggest that mantle of diverse provenance is present beneath the Kerguelen Islands. The results also indicate that the northern part of the Kerguelen Plateau is partially composed of lithospheric mantle derived from the Gondwanaland continents and is not completely oceanic in origin.

REFERENCES AND NOTES

1. H. Whitechurch, R. Montigny, J. Sevigny, M. Storey, V. J. M. Salters, *Proc. Ocean Drill. Prog. Sci. Res.* **120**, 71 (1992); M. S. Pringle, M. F. Coffin, M. S. Storey, *Eos* **78**, 728 (1997).
2. H. L. Davies *et al.*, *Contrib. Mineral. Petrol.* **103**, 457 (1989); M. Storey *et al.*, *Nature* **338**, 574 (1989).
3. The southern Kerguelen Plateau is one of the earliest known products of the extensive Kerguelen plume magmatism with dredge samples dated at 109 to 115 million years old (*1*), and rocks from ODP drill-holes range from 112 to 85 Ma [M. Storey, M. S. Pringle, M. F. Coffin, J. Wijbrams, *Eos* **77**, W123 (1996)]. The Ninetyeast Ridge is the hotspot track from the northward migration of India from >83 to 43 Ma [(*32*); R. A. Duncan, *Proc. Ocean Drill. Prog. Sci. Res.* **121**, 507 (1991)]. Broken Ridge and its conjugate, the northern Kerguelen Plateau, were erupted from 88 Ma until 43 Ma (*32*), when rifting was initiated along the Southeast Indian Ridge (SEIR) between Broken Ridge and the northern Kerguelen Plateau [J.-Y. Royer and D. T. Sandwell, *J. Geophys. Res.* **94**, 13 (1989)]. The Kerguelen Islands are the most recent of the Kerguelen Plume volcanism from 39 to 0.04 Ma [(*11*); J. Nougier, in *Antarctic Geology and Geophysics*, R. J. Adie, Ed. (International Union of Geological Sciences, Series B–No. 1, Scandinavian Univ. Books, Oslo, 1972), pp. 803–808].
4. S. R. Hart, *Nature* **309**, 753 (1984); D. Weis and F. A. Frey, *J. Geophys. Res.* **101**, 13 (1996).
5. J. J. Mahoney *et al.*, *ibid.* **94**, 4033 (1989).
6. N. D. Watkins, B. M. Gunn, J. Nougier, A. K. Baksi, *Geol. Soc. Am. Bull.* **85**, 201 (1974); L. Dosso *et al.*, *Earth Planet. Sci. Lett.* **43**, 46 (1979); I. Gautier *et al.*, *ibid.* **100**, 59 (1990); D. Weis, F. A. Frey, H. Leyrit, I. Gautier, *ibid.* **118**, 101 (1993).
7. C. Alibert, *Proc. Ocean Drill. Prog. Sci. Res.* **119**, 293 (1991); J. J. Mahoney *et al.*, *Chem. Geol.* **120**, 315 (1994).
8. S. Operto and P. Charvis, *Geology* **23**, 137 (1995).
9. M. Recq, D. Brefort, J. Malod, J.-L. Veinante, *Tectonophysics* **182**, 227 (1990).
10. Olivine separates and peridotite whole-rock powders were ground in an agate shatterbox vial, prepared for Os analysis by NiS fire-assay and distillation, and measured by negative thermal ionization mass spectrometry at Woods Hole Oceanographic Institution [(*20*); G. Ravizza, *Earth Planet. Sci. Lett.* **118**, 335 (1993)]. On the basis of counting statistics, the precision associated with $^{187}Os/^{188}Os$ ranged from 0.10 to 0.44% (2σ), although replicate analyses (one was a separate aliquot from the same powder split and another from a separate powder split) agreed within ±0.5% and ±0.7%, respectively. Osmium standard runs were reproducible within 0.3% (2σ). Osmium concentrations were determined by fire-assay and isotope dilution and were reproducible at ±7% (2σ). Blank corrections for Os isotopic composition and concentrations were less than the uncertainty of counting statistics in most cases and only applied when the correction was greater than the counting error. Rhenium concentrations were measured on separate powder splits by inductively coupled plasma-mass spectrometry at the Lamont-Doherty Earth Observatory. Reported Re concentrations are not blank-corrected (procedural blank was ~10 to 20 ppt), and counting statistics were 0.6 to 3.2% (2σ). Thus, most of the samples had negligible amounts of Re.
11. A. Giret and J. Lameyre, in *Antarctic Earth Science*, R. L. Oliver *et al.*, Eds. (Cambridge Univ. Press Cambridge, 1983), pp. 646–651; K. Nicolaysen *et al.*, *Eos* **77**, 824 (1996).
12. D. R. Hassler and N. Shimizu, *Eos* **75**, 710 (1994); D. R. Hassler and N. Shimizu, in preparation.
13. A. Michard, R. Montigny, R. Schlich, *Earth Planet. Sci. Lett.* **78**, 104 (1986); L. Dosso *et al.*, *ibid.* **88**, 47 (1988).
14. N. Mattielli *et al.*, *Lithos* **37**, 261 (1996).
15. J. W. Morgan, *J. Geophys. Res.* **91**, 12 (1986); S. R. Hart and G. E. Ravizza, in *Earth Processes: Reading the Isotopic Code*, A. Basu and S. R. Hart, Eds. (American Geophysical Union, Washington, DC, 1996), vol. 95, pp. 123–134.
16. R. J. Walker, R. W. Carlson, S. B. Shirey, F. R. Boyd, *Geochim. Cosmochim. Acta* **53**, 1583 (1989).
17. E. H. Hauri, thesis, Massachusetts Institute of Technology–Woods Hole Oceanographic Institution (1992).
18. H.-J. Yang *et al.*, *J. Petrol.*, in press.
19. C. E. Martin, *Geochim. Cosmochim. Acta* **55**, 1421 (1991).
20. E. H. Hauri and S. R. Hart, *Earth Planet. Sci. Lett.* **114**, 353 (1993).
21. E. Widom and S. B. Shirey, *ibid.* **142**, 451 (1996).
22. L. Reisberg *et al.*, *ibid.* **120**, 149 (1993).
23. E. H. Hauri, *Nature* **382**, 415 (1996).
24. M. Roy-Barman and C. J. Allègre, *Geochim. Cosmochim. Acta* **58**, 5043 (1994); J. E. Snow and L. Reisberg, *Earth Planet. Sci. Lett.* **133**, 411 (1995).
25. The T_{RD} model age is a special case of the Re-Os model age (T_{MA}) and is defined as the time at which the Os isotopic composition of the sample intersects a chondritic Re-Os mantle evolution curve, and the Re/Os ratio of the sample is 0. That is,

$$T_{MA} = \frac{1}{\lambda} \times \ln\left[\frac{\left(\frac{^{187}Os}{^{188}Os}\right)_{Mantle} - \left(\frac{^{187}Os}{^{188}Os}\right)_{Sample}}{\left(\frac{^{187}Re}{^{188}Os}\right)_{Mantle} - \left(\frac{^{187}Re}{^{188}Os}\right)_{Sample}} + 1\right]$$

where λ is the decay constant for ^{187}Re [1.59×10^{-11}; M. Lindner *et al.*, *Nature* **320**, 246 (1986)] and $(^{187}Os/^{188}Os)_{Mantle}$ = 0.12757 and $(^{187}Re/^{188}Os)_{Mantle}$ = 0.39716 from the mean of carbonaceous chondrites as originally defined by Walker *et al.* (*16*). This age is a minimum because it assumes that Re is completely removed during the melting event that formed these rocks. There is some uncertainty as to the exact Re/Os ratio of Earth's mantle. Present day $(^{187}Os/^{188}Os)_{Mantle}$ may be as unradiogenic as some abyssal peridotites [~0.122 (*24*)] in which case the model ages decrease, or more radiogenic as estimated from fertile xenoliths [~0.1290; T. Meisel, R. J. Walker, J. W. Morgan, *Nature* **383**, 517 (1996)], where model ages would be even older. Most estimates of $(^{187}Os/^{188}Os)_{Mantle}$ are between 0.124 and 0.130 (*19*, *24*), and the use of either extreme does not affect our conclusions. Ancient $(^{187}Os/^{188}Os)_{Mantle}$ is better defined because of iron meteorite initial ratios [M. F. Horan, J. W. Morgan, R. J. Walker, J. N. Grossman, *Science* **255**, 1118 (1992)], and because ingrowth of ^{187}Os was still small. The T_{MA} for most samples are within the estimates for T_{RD} because of the samples' low Re contents. Ages were omitted for those samples giving future ages, or samples whose $^{187}Os/^{188}Os$ values are similar to the estimated range of $(^{187}Os/^{188}Os)_{Mantle}$.
26. L. Reisberg and J.-P. Lorand, *Nature* **376**, 159 (1995); T. Meisel, G. G. Bino, T. F. Nägler, *Geochim. Cosmochim. Acta* **60**, 2583 (1996).
27. R. W. Carlson and A. J. Irving, *Earth Planet. Sci. Lett.*

126, 457 (1994); D. G. Pearson *et al.*, *ibid.* **134**, 341 (1995); D. G. Pearson *et al.*, *Geochim. Cosmochim. Acta* **59**, 959 (1995).
28. S. B. Shirey, J. F. Bender, C. H. Langmuir, *Nature* **325**, 217 (1987); C. J. Hawkesworth, M. S. M. Mantovani, P. N. Taylor, Z. Palacz, *ibid.* **322**, 356 (1986); J. Mahoney, A. P. LeRoex, Z. Peng, R. L. Fisher, J. H. Natland, *J. Geophys. Res.* **97**, 19 (1992); J. J. Mahoney, W. M. White, B. G. J. Upton, C. R. Neal, R. A. Scrutton, *Geology* **24**, 615 (1996).
29. R. S. White, *Nature* **327**, 191 (1987); _____ and D. McKenzie, *J. Geophys. Res.* **94**, 7685 (1989).
30. F. A. Frey *et al.*, *Earth Planet. Sci. Lett.* **144**, 163 (1996).
31. R. D. Müller, J.-Y. Royer, L. A. Lawver, *Geology* **21**, 275 (1993); B. C. Storey, *Nature* **377**, 301 (1995).
32. R. A. Duncan, *J. Volcan. Geotherm. Res.* **4**, 283 (1978).
33. The variation of $^{187}Os/^{188}Os$ and Os concentration do not appear to correlate with any petrographic features or incompatible trace-element abundances.
34. Our samples were collected during the 1992 to 1993 austral field season. We thank A. Giret, F. Frey, D. Weis, and J.-Y. Cotin for assistance in sampling. We also thank G. Ravizza for discussions, S. Hart for sharing of laboratory facilities, J. Blusztajn for advice, K. Burrhus for technical support, E. Nakamura for Sr isotopic analysis of OB93-78 cpx, and F. Frey and M. F. Roden for comments. N.S. acknowledges support from the National Geographic Society (4629-91) and the National Science Foundation (EAR-9219158 and OPP-9417806). This research is also supported by a Cecil and Ida Green Fellowship to D.R.H.

21 January 1998; accepted 26 February 1998

Unitary Control in Quantum Ensembles: Maximizing Signal Intensity in Coherent Spectroscopy

S. J. Glaser,* T. Schulte-Herbrüggen, M. Sieveking, O. Schedletzky, N. C. Nielsen, O. W. Sørensen, C. Griesinger*

Experiments in coherent magnetic resonance, microwave, and optical spectroscopy control quantum-mechanical ensembles by guiding them from initial states toward target states by unitary transformation. Often, the coherences detected as signals are represented by a non-Hermitian operator. Hence, spectroscopic experiments, such as those used in nuclear magnetic resonance, correspond to unitary transformations between operators that in general are not Hermitian. A gradient-based systematic procedure for optimizing these transformations is described that finds the largest projection of a transformed initial operator onto the target operator and, thus, the maximum spectroscopic signal. This method can also be used in applied mathematics and control theory.

The development of specific sets of controlling unitary transformations (pulse sequences) has long been a major thrust in nuclear magnetic resonance (NMR) spectroscopy (*1*) and, more recently, in electron magnetic resonance spectroscopy (*2*), laser coherent control (*3*), and quantum computing (*4*). These spectroscopic experiments are most often applied to quantum ensembles rather than individual atoms or molecules. For example, a test tube of water may contain some 10^{22} hydrogen atoms, and a full quantum-mechanical description would afford $2^{10^{22}}$ spin energy levels; yet, a reduced density operator treatment (*5*, *6*) with no more than four highly averaged matrix elements gives an excellent description of its spin dynamics.

In sufficiently large quantum ensembles, the expectation values of noncommuting operators, such as I_x and I_y, can be determined simultaneously with negligible mutual interference. For example, in NMR it has been customary to record the magnetization from an ensemble along the x and y axes simultaneously in the rotating frame. The complex superposition of the two signals is called quadrature detection and corresponds to the non-Hermitian detection operator $I^+ = I_x + iI_y$ (*1*) (where $i = \sqrt{-1}$). Moreover, non-Hermitian components of the density operator, such as I^+, can be distinguished experimentally from their adjoints (in this case from I^-) by their different responses to rotations around the quantization axis z. This makes them amenable to filtering by pulsed field gradients and coherence transfer echoes and also results in opposite signs of their oscillation frequencies during evolution or detection periods. Consider, for example, a standard two-dimensional (2D) NMR experiment with an evolution period t_1 and a detection period t_2. In order to maximize the intensity of 2D peaks, two successive transformations must be optimized. In a first step, the density operator containing the operators I_z that represent the ensemble of nuclear spins at thermal equilibrium is transformed into a state including non-Hermitian operators like I^+ or products of such operators oscillating during t_1. In a second step, these non-Hermitian operators must be transformed to yield non-Hermitian operators I^- that are detected by I^+ during t_2. Almost all multidimensional NMR experiments require optimal transfers between operators that are in general not Hermitian. A procedure to find unitary transformations of a given operator A achieving the largest projection onto a target operator C (where both may take the form of an arbitrary complex square matrix) is highly desired not only by the experimentalist; in this general case, it has so far also been an unsolved problem to the mathematicians (*7*).

In this context, we address the following questions. (i) What are the unitary transformations of a given initial operator A that maximize the transfer amplitude onto a target operator C, and what is the maximum amplitude? (ii) What additional restrictions are imposed by symmetry or a limited set of experimentally available control fields?

For the transformation between an initial quantum-mechanical state function $|\psi_i\rangle$ and a target state function $|\psi_t\rangle$ of the same norm, it is always possible to find a unitary operator U that converts $|\psi_i\rangle$ completely into $|\psi_t\rangle$, that is, $U|\psi_i\rangle = b|\psi_t\rangle$ with $b = 1$. In this case, the transfer amplitude is only restricted by experimental constraints (*8*). This argument also holds for an ensemble in a pure state where all individual quantum systems can be described by the same state function $|\psi\rangle$. However, the situation is quite different for nonpure states. Suppose the operator A represents a (not necessarily Hermitian) component of the density operator (*5*, *6*) relevant to a specific signal in a spectroscopic experiment. If relaxation and other dissipative processes can be neglected, A is transformed during the experiment by a unitary transformation of the form

$$\tilde{A} = UAU^\dagger \qquad (1)$$

where the propagator U is a unitary operator (*9*). In contrast to unitary transformations between two normalized state functions $|\psi_i\rangle$ and $|\psi_t\rangle$, it is in general not possible to transform an arbitrary initial

S. J. Glaser, O. Schedletzky, C. Griesinger, Institut für Organische Chemie, J. W. Goethe-Universität, Marie-Curie-Strasse 11, D-60439 Frankfurt, Germany.
T. Schulte-Herbrüggen, Laboratorium für Physikalische Chemie, ETH Zentrum, CH-8092 Zürich, Switzerland.
M. Sieveking, Institut für Angewandte Mathematik, J. W. Goethe-Universität, Robert-Mayer-Strasse 6-10, D-60439 Frankfurt, Germany.
N. C. Nielsen, Instrument Center for Solid-State NMR Spectroscopy, Department of Chemistry, University of Aarhus, Langelandsgade 140, DK-8000 Aarhus C, Denmark.
O. W. Sørensen, Department of Chemistry, Carlsberg Laboratory, Gamle Carlsberg Vej 10, DK-2500 Valby, Denmark.

*To whom correspondence should be addressed. E-mail: sg@org.chemie.uni-frankfurt.de (S.J.G.) and cigr@org.chemie.uni-frankfurt.de (C.G.)